NASA Technical Memorandum 108855

Dynamics of the McDonnell Douglas Large Scale Dynamic Rig and Dynamic Calibration of the Rotor Balance

Khanh Nguyen and Benton Lau, Ames Research Center, Moffett Field, California

October 1994

National Aeronautics and
Space Administration

Ames Research Center
Moffett Field, California 94035-1000

NOMENCLATURE

C_r	modal damping, lb-sec/ft
C_T	rotor thrust coefficient
H	transfer matrix relating the vibratory hub loads to the balance signals; inverse of the dynamic calibration matrix
$\hat{H}$	complex representation of H
i	$\sqrt{-1}$
Im	imaginary part of a complex number
K_r	modal stiffness, lb/ft
M_r	modal mass, slug
nP	n-per-rev *or* n per rotor revolution
Re	real part of a complex number
s	frequency response of shaker excitation, complex scalar, lb
u_i	input vector indicating type of shake, complex constant
$\hat{u}_i$	frequency response of input vector, complex
U	real representation of $\hat{U}$
$\hat{U}$	input matrix with column u_i, complex
v	vector of uncorrected five-per-rev balance signal components, real
w	vector of corrected five-per-rev hub load components, real
y_i	frequency response vector of balance transfer functions, complex
$\hat{y}_i$	frequency response vector of balance channels, complex
Y	real representation of $\hat{Y}$
$\hat{Y}$	response matrix with column y_i, complex

ζ_r	modal damping ratio, percent critical
μ	advance ratio
ϕ_Z	phase of complex number Z
σ	rotor solidity
Ψ	rotor azimuth, positive counterclockwise as viewed from above, deg
ω_0	nominal five-per-rev of the MDART rotor, ω_0= 32.67 Hz
ω_r	modal frequency, rad/sec
$\|Z\|$	magnitude of complex number Z
$[\ldots]^{-1}$	inverse of matrix [...]
$[\ldots]^T$	transpose of matrix [...]

Abbreviations

AF	axial force, positive aft, lb
NF	normal force, positive up, lb
PM	pitching moment, positive nose up, in.-lb
RM	rolling moment, positive advancing side down, in.-lb
SF	side force, positive toward advancing side, lb

Subscripts

c	cosine component
s	sine component

Superscripts

c	dynamically corrected hub load components
u	dynamically uncorrected hub load components

DYNAMICS OF THE McDONNELL DOUGLAS LARGE SCALE DYNAMIC RIG AND DYNAMIC CALIBRATION OF THE ROTOR BALANCE

Khanh Nguyen and Benton Lau

Ames Research Center

SUMMARY

A shake test was performed on the Large Scale Dynamic Rig in the 40- by 80-Foot Wind Tunnel in support of the McDonnell Douglas Advanced Rotor Technology (MDART) Test Program. The shake test identifies the hub modes and the dynamic calibration matrix of the rotor balance. For hub mode identification, three configurations were tested: wind tunnel scale unlocked with dampers engaged and disengaged, and wind tunnel scale locked. Test data were analyzed with a multi-degree-of-freedom time domain algorithm to identify the modal properties of the hub modes. The damping of the low frequency hub modes (ground resonance modes) increases significantly with the wind tunnel dampers engaged. For dynamic calibration of the rotor balance, the shake test was performed only with the wind tunnel dampers engaged. The dynamic calibration matrix, computed from the shake test data using a least squares error method, is used to correct the five-per-rev vibratory balance readings. The corrections are large for the side force, moderate for the axial force and inplane hub moments, and small for the normal force.

INTRODUCTION

In support of the McDonnell Douglas Advanced Rotor Technology (MDART) Test Program, a shake test was conducted on the Large Scale Dynamic Rig (LSDR) in the 40- by 80-Foot Wind Tunnel. The MDART Test Program is a joint cooperative effort between NASA Ames Research Center and McDonnell Douglas Helicopter Systems to evaluate the aerodynamic performance and the aeromechanic properties of the MDART rotor. The MDART rotor is a modern five-bladed bearingless design that incorporates elastomeric dampers to augment the inplane blade motion damping. The objectives of the shake test are to identify the modal parameters of the inplane hub modes and to perform a dynamic calibration of the rotor balance. This report describes the shake test setup, testing procedure, data acquisition and reduction process, and the shake test results.

The first objective of the shake test is to identify the modal properties of the hub inplane motions. The prediction of the ground resonance for the rotor-support system is a crucial part of the risk reduction process in rotor testing. Such analysis requires the structural properties of the hub modes as input. In particular, ground resonance is an aeromechanic instability that can occur during the frequency-crossings of the inplane hub and blade motions. Since the frequency of the blade inplane mode varies with the rotor rotational speed, the frequency-crossings define the critical speed ranges in rotor operation. Ground resonance depends on the level of damping of the blade inplane

modes as well as the damping of the hub modes, which in turn depends on the structural properties of the stand support system. Several configurations of the wind tunnel setup were shake-tested to identify a ground resonance-safe test configuration.

The second objective of the shake test is to perform a dynamic calibration of the rotor balance. Accurate measurement of the rotor vibratory hub loads is crucial in the development of rotor systems and has remained one of the major challenges in rotorcraft testing (refs. 1–4). In the MDART test setup, a five-component rotor balance installed below the rotor hub in the nonrotating system measures both the steady and the vibratory rotor hub loads. Since the measured vibratory hub loads are modulated by the dynamics of the rotor balance and the model support system, the results of the dynamic calibration identify the transfer functions relating the actual applied vibratory hub loads to the balance readings. Furthermore, since the frequency contents of the rotor vibratory hub loads in forward flight are dominated by the blade number harmonics, the dynamic calibration focuses on the balance frequency responses at the nominal five-per-rev (5P) of the MDART rotor.

TEST SYSTEM DESCRIPTION

Test Setup

Figure 1 shows the LSDR installed in the test section of the 40- by 80-Foot Wind Tunnel. The LSDR consists of an upper and a lower housing connected by a vertical stand strut. In the upper housing, the rotor hub is connected to a static mast which is mounted to a five-component rotor balance. The rotor balance consists of an upper and a lower ring connected by four strain gauge instrumented flexures of rectangular cross section. The vertical distance between the rotor hub and the balance center is 37 inches. The static mast encloses the rotating drive shaft that transfers torque directly to the rotor hub. In this arrangement, the static mast allows a direct transfer of the rotor hub shears and moments to the rotor balance in the nonrotating system. The upper fairing encloses the balance housing, the hydraulic servo-actuators for the rotor control system, and the static mast.

A vertical stand strut connects the upper balance housing to the lower housing and is placed on top of the transmission. The transmission and a 1,500-hp General Electric motor are mounted to a sled. The sled is a major structural component supporting the lower housing. A large lower fairing encloses the sled, the motor, and the transmission. The front cross-arm extends from the base of the vertical stand and rests on two 2-foot front struts and a 60-inch tip. Another arm extends rearward from the end of the sled and rests on a telescoping tail strut that controls changes in the model longitudinal shaft tilt. A rectangular floating frame supports the test section turntable which in turn supports the three struts.

The four lift posts of the wind tunnel scale support the floating frame. The scale is the balance system for the wind tunnel, designed to measure the loads acting on the test model as well as the supporting structures. The lift posts measure the vertical loads, while the two side force piers and the drag pier measure the inplane loads. The moments can be derived from the forces measured with the lift posts and the side force piers due to the unique arrangement of these instruments. Since the lift posts and the piers are designed for load measurements, the scale provides little stiffness and

damping to the support model. As a safety measure, the scale can be locked out to stiffen the support system, or, in the unlocked configuration, operates with the balance dampers engaged. The scale is inoperative in the locked configuration. In the unlocked configuration, the balance dampers provide additional damping to the support system.

A close-up photo of a vertical shake is shown in figure 2. Only the blade flexbeams and the snubbers are installed during the shake test. The missing components from the MDART rotor are the blades, the dampers, and the pitchcases. For hub mode identification, a lead weight is attached to the hub to simulate the rotor mass. For dynamic calibration, a circular plate (fig. 2) is mounted to the hub to simulate the rotor weight and to allow off-shaft axis vertical shaking. The plate is sufficiently rigid and properly supported to prevent either elastic deformation or rigid body motion during actuator excitation.

The MTS Model 204.08 hydraulic actuator is used to excite the simulated hub as shown in figure 2 for a vertical shake and in figure 3 for an inplane shake. The MTS Model 406.11 shaker controller, operated in the stroke feedback mode, provides excitation signals to the actuator. For inplane shake, the rear end of the actuator is attached to a 5-foot extension arm supported by an 11,600-lb reaction mass. For vertical shake, the rear end of the actuator is supported by the reaction mass directly. In both cases, the reaction mass is hung from a gantry crane. The front end of the actuator is attached to a load cell, which is connected to the dummy hub, to monitor the actuator force. The shaker is aligned with respect to either the extension arm or the actuator, which in turn is aligned parallel to each of the shaking directions. After rough alignment of the actuator and the extension arm using the gantry crane, fine alignment is achieved by applying tension to the guy wires attaching the reaction mass to the tunnel floor. The guy wires also restrain the reaction mass from swinging during actuator excitation.

Instrumentation and Data Acquisition

The instrumentation includes fifteen accelerometers, the load cell, and the five components of the rotor balance. The accelerometers are mounted at seven locations on the test stand to identify the types of hub modes. Figure 4 depicts the accelerometer locations with a stick model of the test stand, and table 1 provides the nodal coordinates of the stick model. Note that the origin of the Cartesian coordinate is the intersection of line 1-7 and line 5-6 shown in figure 4. Three accelerometers are mounted at the hub (node 1) to measure the hub vertical, longitudinal, and lateral responses. The other six pairs of accelerometers are mounted at the top and bottom of the two front struts (nodes 3–6) as well as the tail strut (nodes 8 and 10) to measure the strut responses in the longitudinal and lateral directions. The five components of the rotor balance are the axial, side, and normal forces, and the pitching and rolling moments. The load cell is calibrated up to ±1,000 lb, while the accelerometers are calibrated to ±1 g at frequencies up to 100 Hz.

The selection of which signals to record depends on the objective of the shake test. The recorded signals include all fifteen accelerometers and the load cell for the hub mode identification and all five rotor balance channels and the load cell for the dynamic calibration.

The GenRad Model 2515 Computer-Aided Test System acquires the data and computes the transfer functions using the Real Time Analysis (RTA) program. The GenRad is a portable dynamic signal analyzer for general purpose data acquisition and analysis. The data acquisition is capable of acquiring up to 16 channels and analyzing data in the frequency ranges up to 25.6 kHz with anti-alias protection on all channels. The computed transfer function relates either an accelerometer or a balance channel frequency response to the load cell input. The computed transfer functions are subsequently stored in the GenRad database.

The response function bandwidth is set to 16 Hz for hub mode identification and to 64 Hz for balance calibration. The frequency spectrum consists of 512 spectral lines. For hub mode identification, only the modes with frequency content less than the rotor one-per-rev (6.53 Hz) affect the ground resonance behaviors of the rotor-support system. For dynamic calibration, the frequency of interest is the 5P of the MDART rotor, which is 32.67 Hz. The frequency estimates are based on the nominal operating rpm of 392. During the data acquisition, a Hanning window is applied to all channels to minimize leakage. The shaker controller receives broadband random frequency signals generated by the GenRad to drive the hydraulic actuator. The average excitation levels are 80 lb for hub mode identification and 250 lb for dynamic calibration. Subsequent results from the dynamic calibration indicate that the excitation level should have been more than double for the calibration of the vibratory axial force. A linear time-averaging scheme is employed in the computation of the transfer functions to improve the signal-to-noise ratio.

Test Procedure

Hub mode identification– For hub mode identification, the shaker supplied two independent inplane excitations in the longitudinal and lateral directions for each of the three wind tunnel configurations: wind tunnel scale unlocked with dampers off and dampers on, and wind tunnel scale locked. Since preliminary results from the ground resonance prediction using the shake test data indicated that safe rotor operation was ensured with the wind tunnel dampers engaged, the dynamic calibration was performed only in the dampers-on configuration.

Dynamic calibration– The dynamic calibration of the rotor balance is performed with seven independent shakes. In fact, only five independent shakes are necessary to determine the dynamic calibration matrix. However, seven shakes are performed to reduce experimental uncertainties. The dynamic calibration is conducted with the rotor shaft vertical and nonrotating. The effects of the rotor shaft tilt on the dynamic calibration, which can be significant (ref. 4), are not investigated. The effects of shaft rotation on the dynamic calibration are expected to be small, as shown in reference 4 for another full-scale rotor balance system, because of the unique arrangement of the rotor test stand that allows a direct transfer of rotating hub loads to the fixed system through a static mast.

The seven shaking configurations include two inplane shakes and five vertical shakes. The inplane shakes in the longitudinal and lateral directions provide pure axial force and side force inputs, respectively. Figure 3 shows the setup for a pure side force excitation. One of the vertical shakes is at the hub center, providing a pure vertical force input. The 28-inch diameter circular plate allows for the other four off-axis vertical shakes for combined vertical force-inplane hub moment input, one of which is shown in figure 2. For the off-axis vertical shakes, the excitation is applied

near the edge of the circular plate resulting in an offset of 13.8 inches from the hub centerline. Off-axis vertical shakes at the fore and aft positions of the plate provide two independent vertical force-pitching moment inputs, while the off-axis vertical shakes at the right and left sides of the plate provide the other two independent vertical force-rolling moment inputs.

DATA ANALYSIS AND TEST RESULTS

Hub Mode Identification

For hub mode identification, the shake test data are postprocessed using the Modal Plus software package (ref. 5) residing on a Micro VAX II computer. The Polyreference method is used to identify modal parameters from the transfer function data. This method is a time-domain, curve-fitting algorithm that provides a global estimate of the modal parameters from multiple reference locations. The modal parameter extraction involves three steps:

Step 1: Specify the response functions and the coordinates of the accelerometer responses and of the shaker. The time-domain impulse response functions, obtained from the inverse Fourier Transform of the response functions, are used to generate a correlation matrix.

Step 2: Plot the error chart that specifies the residual error as a function of the number of roots. Use the error chart to select the smallest number of roots that minimizes the residual errors. Using the selected roots, a matrix polynomial is generated based on the correlation matrix. The roots of the matrix polynomial yield the modal frequencies and damping, while the eigenvectors provide information to compute the mode shapes.

Step 3: Generate the residues from a least-squares estimate of the response functions based on the reference locations defined by the correlation matrix. Information about the residues allows computation of the modal mass and stiffness.

Nine hub modes in the frequency range 0–13 Hz are identified from the shake test. The results are shown in table 2 for the three scale configurations: scale unlocked with dampers off and dampers on, and scale locked. The tabulated modal parameters are the natural frequency, critical damping ratio, and the modal mass for each mode. Information from the mode shapes allows identification of the types of modes. These modes include the scale longitudinal and lateral modes, and the stand longitudinal, lateral, and yaw modes. The modal stiffness K_r and modal damping C_r can be computed from the tabulated parameters as

$$K_r = M_r \omega_r^2 \tag{1}$$

$$C_r = 2\zeta_r M_r \omega_r \tag{2}$$

where M_r, ζ_r, and ω_r are the modal mass, damping, and natural frequency (in rad/sec), respectively.

For ground resonance prediction, only the modes with a frequency less than the nominal rotor rotational speed, 6.53 Hz, are required. The results indicate the scale longitudinal mode is absent with the dampers engaged, while both scale modes are absent in the locked position. Within the frequency range of data analysis, the fourth longitudinal stand mode is only present with the scale locked. The damping of the ground resonance modes (with frequencies less than 6.53 Hz) increases significantly with the wind tunnel dampers engaged. In fact, the lowest damped mode is the stand first lateral mode with a critical damping ratio of 2 percent. Independent analysis conducted by McDonnell Douglas Helicopter Systems using the identified modal parameters indicates that operation of the MDART rotor is safe from ground resonance with the dampers engaged. From the rotor operation standpoint, the second longitudinal and the yaw stand modes (6.57 and 6.71 Hz, respectively) might be a source vibration problem in this configuration because of their frequency proximity to the rotor nominal rotational speed and their low damped nature. However, the potential resonance did not pose a problem during actual wind tunnel testing, probably because of the large masses of these two modes (see table 2).

Comparing the results of table 2 with those presented in reference 6, a large difference is noted in the frequency of the stand first longitudinal mode; the frequency is significantly higher for the MDART test (4.19 versus 2.80 Hz for the dampers-off configuration). Reference 6 documents the shake test results of the LSDR in support of the Light Helicopter Experimental (LHX) test. Another significant difference is the absence of the balance frame longitudinal mode in the MDART test with the dampers-on configuration (a frequency of 2.32 Hz was measured for this mode during the LHX test). The differences in the two shake tests of the same structure are attributed to the presence of a relatively large tail boom mounted on the upper housing to simulate the LHX fuselage during the previous test. In addition, the sizes of the electric motors, the power sources for the rotors, are different; the MDART test employs a 1,500-hp motor that is significantly heavier and larger than the 600-hp motor used in the LHX test. The differences in the model configuration account for the differences in the modal properties shown in table 2 and those reported in reference 6.

Dynamic calibration–

Mathematical formulation: The fundamental assumption in the analysis of the dynamic calibration is that the balance dynamics are represented by a linear time-invariant system. The input $\hat{u}_i$ represents the hub loads, and the output $\hat{y}_i$ represents the balance readings. Related by a five-by-five transfer function matrix $\hat{H}$, both $\hat{u}_i$ and $\hat{y}_i$ are five-component vectors with elements axial force (*AF*), side force (*SF*), normal force (*NF*), rolling moment (*RM*), and pitching moment (*PM*). The goal of the dynamic calibration is to establish a relationship such that the vibratory hub loads can be determined given the vibratory balance readings. Specifically, the determination of $\hat{H}^{-1}$ establishes the relationship. Starting from the above description, the basic relation is

$$\hat{H}(\omega)\,\hat{u}_i(\omega)=\hat{y}_i(\omega) \tag{3}$$

where the subscript i denotes a sequence in the shake test, each corresponding to the type of shaking input. Table 3 presents the seven sequences of the shake test. Since only one shaker was used during the shake test, the shaker excitation can be factored from $\hat{u}_i(\omega)$ as

$$\hat{H}(\omega)\, u_i\, s(\omega) = \hat{y}_i(\omega) \tag{4}$$

where $s(\omega)$ is the frequency response of the shaker input as measured by the load cell, and u_i is a complex constant vector that denotes the types of shake and the shaking directions. Note that u_i is defined as complex only for consistency with the above relation even though the elements of u_i are real. For a pure side force excitation corresponding to the first sequence, u_1 has the form:

$$u_1^T = [0 \quad -1 \quad 0 \quad 0 \quad 0] \tag{5}$$

A nonzero second entry indicates a side force excitation, and the negative sign indicates the excitation is applied in the negative side force direction. As another example, an off-axis vertical shake, such as in sequence 7, has both vertical force and rolling moment excitation, and the input vector u_7 is

$$u_7^T = [0 \quad 0 \quad 1 \quad 13.8 \quad 0] \tag{6}$$

The nonzero third entry indicates a vertical force input, while the numerical value of the fourth entry denotes the moment arm offset (in inches) for the rolling moment input.

Dividing both sides of equation 4 by $s(\omega)$ leads to

$$\hat{H}(\omega) u_i = y_i(\omega) \tag{7}$$

where the components of y_i are the transfer functions of the balance channels obtained on line during the shake test. With this description, y_i can be expressed as

$$y_i^T(\omega) = \left[\frac{AF}{s}(\omega) \quad \frac{SF}{s}(\omega) \quad \frac{NF}{s}(\omega) \quad \frac{RM}{s}(\omega) \quad \frac{PM}{s}(\omega)\right] \tag{8}$$

Combining all seven shake results into equation 7 yields

$$\hat{H}(\omega)[u_1 \quad u_2 \ldots u_6 \quad u_7] = [y_1(\omega) \quad y_2(\omega) \ldots y_6(\omega) \quad y_7(\omega)] \tag{9}$$

or

$$\hat{H}(\omega)\hat{U} = \hat{Y}(\omega) \tag{10}$$

where both $\hat{U}$ and $\hat{Y}$ are five-by-seven complex matrices. Note that $\hat{H}$ is a five-by-five complex matrix that relates the vibratory hub loads to the vibratory balance signals. Before solving for $\hat{H}$, a mathematical method adapted from reference 7 is used to facilitate the manipulation of complex matrices. This method allows the representation of a complex number by a two-by-two real matrix

$$\mathrm{Re}+i\,\mathrm{Im} \sim \begin{bmatrix} \mathrm{Re} & -\mathrm{Im} \\ \mathrm{Im} & \mathrm{Re} \end{bmatrix} \tag{11}$$

where Re and Im denote the real and imaginary parts of a complex number, respectively; $i = \sqrt{-1}$; and ~ denotes an equivalent relation. This antisymmetric matrix consists of the real part on the diagonal and the imaginary part with opposite signs on the off-diagonal. For real numbers, such as the entries of matrix $\hat{U}$, the off-diagonal terms are simply zero. With this representation, complex arithmetic is essentially replaced with matrix manipulation. This complex-to-real operation doubles the size of the three matrices $\hat{H}$, $\hat{U}$, and $\hat{Y}$, resulting in three real matrices: H of size ten-by-ten, and U and Y of size ten-by-fourteen each. With this representation, equation 10 can be expressed as

$$H(\omega)U = Y(\omega) \tag{12}$$

from which, the least squares solution of H is

$$H(\omega) = Y(\omega)U^T(UU^T)^{-1} \tag{13}$$

Dynamic calibration results: In helicopter rotors, the frequency content of the vibratory hub loads is dominated by the blade-number harmonics, which is 5P for the five-bladed MDART rotor. Therefore, the dynamic calibration focuses only on the numerical value of H at 32.67 Hz, or ω_0, corresponding to the nominal rotor rpm of 392. From the shake test results, the numerical values of Y at ω_0 are

.03	−.06	−.21	−1.53	.03	.02	−.07	−.71	.19	.66	−.07	.03	.19	−.13
.06	.03	1.53	−.21	−.02	.03	.71	−.07	−.66	.19	−.03	−.07	.13	.19
3.46	−1.30	.07	−.01	.10	.00	−.05	−.06	−.06	.01	1.80	−.31	−1.76	.38
1.30	3.46	.01	.07	.00	.10	.06	−.05	−.01	−.06	.31	−1.80	−.38	−1.76
−.06	−.25	−.11	.05	.88	.04	.74	.04	1.03	.05	.82	−.06	.96	.16
.25	−.06	−.05	−.11	−.04	.88	−.04	.74	−.05	1.03	.06	.82	−.16	.96
95.8	−77.9	4.13	3.39	3.16	−.66	−2.64	−2.35	−.86	.97	47.9	−19.2	−46.5	23.3
77.9	95.8	−3.39	4.13	.66	3.16	2.35	−2.64	−.97	−.86	19.2	47.9	23.3	−46.5
5.38	−1.71	−61.6	−65.4	3.40	.61	−42.3	−40.8	46.0	36.0	−.82	1.70	5.35	−5.92
1.71	5.38	65.4	−61.6	−.61	3.40	40.8	−42.3	−36.0	46.0	−1.70	−.82	5.92	5.35

and

$$U = \left[\begin{array}{cc|cc|cc|cc|cc|cc|cc} 0 & 0 & -1 & 0 & 0 & 0 & 0 & 0 & 0 & 0 & 0 & 0 & 0 & 0 \\ 0 & 0 & 0 & -1 & 0 & 0 & 0 & 0 & 0 & 0 & 0 & 0 & 0 & 0 \\ \hline -1 & 0 & 0 & 0 & 0 & 0 & 0 & 0 & 0 & 0 & 0 & 0 & 0 & 0 \\ 0 & -1 & 0 & 0 & 0 & 0 & 0 & 0 & 0 & 0 & 0 & 0 & 0 & 0 \\ \hline 0 & 0 & 0 & 0 & 1 & 0 & 1 & 0 & 1 & 0 & 1 & 0 & 1 & 0 \\ 0 & 0 & 0 & 0 & 0 & 1 & 0 & 1 & 0 & 1 & 0 & 1 & 0 & 1 \\ \hline 0 & 0 & 0 & 0 & 0 & 0 & 0 & 0 & 0 & 0 & 13.8 & 0 & -13.8 & 0 \\ 0 & 0 & 0 & 0 & 0 & 0 & 0 & 0 & 0 & 0 & 0 & 13.8 & 0 & -13.8 \\ \hline 0 & 0 & 0 & 0 & 0 & 0 & -13.8 & 0 & 13.8 & 0 & 0 & 0 & 0 & 0 \\ 0 & 0 & 0 & 0 & 0 & 0 & 0 & -13.8 & 0 & 13.8 & 0 & 0 & 0 & 0 \end{array}\right]$$

Note that the matrices have been partitioned for clarity. Furthermore, since H relates the hub loads to the balance signals, H is by definition the inverse of the dynamic calibration matrix. The dynamic calibration matrix is given by

$$H^{-1}(\omega_0) = \left[\begin{array}{cc|cc|cc|cc|cc} .54 & -1.74 & -.02 & -.74 & .05 & .06 & -.01 & .02 & -.02 & .01 \\ 1.74 & .54 & .74 & -.02 & -.06 & .05 & -.02 & -.01 & -.01 & -.02 \\ \hline -.35 & -.43 & .64 & 1.00 & .01 & .0 & -.01 & -.04 & .0 & .01 \\ .43 & -.35 & -1.00 & .64 & .0 & .01 & .04 & -.01 & -.01 & .0 \\ \hline .17 & -.22 & .20 & .09 & 1.13 & -.06 & -.01 & .0 & -.01 & .0 \\ .22 & .17 & -.09 & .20 & .06 & 1.13 & .0 & -.01 & .0 & -.01 \\ \hline -10.75 & -10.61 & 30.05 & 25.70 & .12 & .09 & -.60 & -1.02 & .03 & .19 \\ 10.61 & -10.75 & -25.70 & -30.05 & -.09 & .12 & 1.02 & -.60 & -.19 & .03 \\ \hline -16.50 & 36.80 & 2.32 & 13.07 & -1.13 & -.55 & .03 & -.41 & .61 & -.37 \\ -36.80 & -16.50 & -13.07 & 2.32 & .55 & -1.13 & .41 & .03 & .37 & .61 \end{array}\right]$$

Note that the dynamic calibration matrix retains the same structure as that of U and Y; that is, H^{-1} is composed of two-by-two antisymmetric submatrices with equal entries on the diagonal. This fact implies that the dynamic calibration matrix can be expressed as a five-by-five block or complex matrix, since each two-by-two submatrix can be represented by a complex number. In terms of magnitude and phase (denoted by $Mag\angle Phase$(deg)), the complex form of the dynamic calibration matrix is

$$\hat{H}^{-1} = \left[\begin{array}{ccccc} 1.82\angle 72.8 & 0.74\angle 91.2 & 0.08\angle -46.1 & 0.02\angle -104.4 & 0.02\angle -146.5 \\ 0.55\angle 129. & 1.18\angle -57.4 & 0.01\angle -37.2 & 0.04\angle 110. & 0.01\angle -87.1 \\ 0.28\angle 53.0 & 0.23\angle -24.8 & 1.13\angle 2.82 & 0.01\angle 157.3 & 0.01\angle -152. \\ 15.1\angle 135. & 39.54\angle -40.5 & 0.15\angle -36.4 & 1.18\angle 120.4 & 0.20\angle -80.7 \\ 40.33\angle -114. & 13.27\angle -79.9 & 1.26\angle 154. & 0.41\angle 86.1 & 0.71\angle 31.5 \end{array}\right]$$

In terms of the balance channels, $\hat{H}^{-1}$ can be expressed as

$$\hat{H}^{-1} = \left[\begin{array}{c|c|c|c|c} AF/AF & AF/SF & AF/NF & AF/RM & AF/PM \\ \hline SF/AF & SF/SF & SF/NF & SF/RM & SF/PM \\ \hline NF/AF & NF/SF & NF/NF & NF/RM & NF/PM \\ \hline RM/AF & RM/SF & RM/NF & RM/RM & RM/PM \\ \hline PM/AF & PM/SF & PM/NF & PM/RM & PM/PM \end{array}\right]$$

The diagonal elements represent the dynamic corrections for the primary balance components, while the off-diagonal elements denote the dynamic correction for the interactions. The units of the force/moment components are 1/inch, while those for the moment/force components are inches. The remaining components are dimensionless. Comparing the above matrix with the magnitude components of the dynamic calibration matrix, all primary balance signals except for the pitching moment have an amplification factor greater than one. The interactions between the side force and axial force are moderate (0.74 and 0.55), while the interactions between either the side force or the axial force with the other components are small (less than 0.08). The normal force has small interaction with the other components of the rotor balance (less than 0.3). The interactions between pitching moment-axial force and rolling moment-side force are large and reflect the vertical offset of 37 inches between the hub center and the balance moment center. Note that the amplitudes of these two interaction terms are 40.33 and 39.54, respectively. Also, the dynamic effects of the normal force on the rolling or pitching moments are negligible.

The existence of a pole or zero of H at or near ω_0 can make the dynamic calibration matrix ill-conditioned. Visual inspection of all 25 scalar transfer functions $y_i(\omega)$ can qualitatively determine this condition. However, a rigorous mathematical approach, adopted from reference 7, can quantify the relative closeness of ω_0 to the poles or zeroes of H. This approach is based on the two facts that (1) the zeroes of a transfer function $H(\omega)$ are the frequencies at which the rank of $H(\omega)$ drops below its normal rank, and (2) the poles of $H(\omega)$ are the zeroes of $H^{-1}(\omega)$ for H square. Since $H(\omega)$ is a transfer function matrix, the poles and zeroes of $H(\omega)$ are not necessarily the poles and zeroes of each elemental transfer function due to potential cancellation between the elements. A singular value decomposition of $H(\omega_0)$ reveals that it has full rank. In fact, these singular values are 123.77, 90.12, 0.89, 0.027, and 0.020 and are double values. Since $H(\omega_0)$ has full rank, its inverse also has full rank. (This fact can be checked from the singular values of $H^{-1}(\omega_0)$ which are simply the reciprocal of those of $H(\omega_0)$.) The fact that both $H(\omega_0)$ and its inverse have full rank implies that ω_0 does not lie in the neighborhood of the zeroes of $H(\omega)$ or $H^{-1}(\omega)$. This condition, together with the second fact, infers that ω_0 is not in the neighborhood of a pole of $H(\omega)$.

Dynamically corrected hub loads: With the dynamic calibration matrix determined, the corrected vibratory hub loads can be obtained from the balance readings. During the MDART test program, the raw dynamic data are sampled at 64 samples per rotor revolution and passed through a four-pole Butterworth filter with a bandwidth setting of 100 Hz. Engineering conversion factors are applied to the raw data to yield the reduced data. At this stage, the reduced data are harmonically analyzed, corrected for filtering effects, and saved in the database. Before applying dynamic corrections, the 5P components of the reduced balance readings are expressed as

$$v^T = \left[AF_c^u \;\; AF_s^u \;\; SF_c^u \;\; SF_s^u \;\; NF_c^u \;\; NF_s^u \;\; RM_c^u \;\; RM_s^u \;\; PM_c^u \;\; PM_s^u\right] \tag{14}$$

where the subscripts c and s refer to the cosine and sine components, respectively, and the superscript u refers to the dynamically uncorrected hub load components. The corrected 5P hub loads are then obtained by multiplying v with the dynamic calibration matrix as

$$H^{-1}v=w \tag{15}$$

where the components of the vector w are the corrected 5P hub loads, and w is expressed as

$$w^T=\left[AF_c^c \;\; AF_s^c \;\; SF_c^c \;\; SF_s^c \;\; NF_c^c \;\; NF_s^c \;\; RM_c^c \;\; RM_s^c \;\; PM_c^c \;\; PM_s^c\right] \tag{16}$$

where the superscript c refers to the dynamically corrected hub load components.

Sample results of the dynamic calibration are presented in figures 5–9. These figures show the variations of the MDART 5P hub loads with the rotor advance ratio at the nominal thrust coefficient-solidity ratio C_T/σ of 0.076. Both corrected magnitudes and phases are shown and compared with the corresponding uncorrected components. The magnitude and phase of a hub load component Z are defined as

$$|Z|=\sqrt{Z_c^2+Z_s^2} \tag{17}$$

$$\phi_Z=\tan^{-1}(Z_s/Z_c) \tag{18}$$

respectively, and the time evolution of Z is expressed as

$$Z(\Psi)=|Z|\cos(5\Psi-\phi_Z) \tag{19}$$

with Ψ being the rotor azimuth.

Figure 5 shows the effects of the dynamic correction on the axial hub force. The magnitude correction of figure 5(a) shows that the correction factor for this component is approximately 1.5 over the whole speed range. Also, the corrected phase leads the uncorrected one by approximately 90 deg. Note that the magnitude correction is not uniform over the speed range shown because the correction includes interactions with other load components. If the interactions are neglected by setting the off-diagonal block matrices of the dynamic calibration matrix to zero, then both the magnitude and the phase corrections would be uniform.

The dynamic corrections for the side force are shown in figure 6. Over the speed range shown, the magnitude of the corrected component is smaller than the uncorrected one, and the difference in amplitude is moderate at the low speed (μ less than 0.15) and becomes significant at the higher speed range. The largest correction occurs at the advance ratio of 0.20 with a reduction of two-thirds in magnitude. The phase correction for the side force is small, except for one data point at μ equal to 0.15 where the corrected phase lags the uncorrected one by 95 deg.

The normal force corrections shown in figure 7 indicate that the dynamic corrections on this force component are small in both magnitude and phase. The magnitude correction is on the order of 20 percent at low speed and decreases at higher speeds, while the phase correction is small at low speeds and increases slightly, up to 20-deg phase lead, at high speeds.

The dynamic corrections for the rolling and pitching moments are shown in figures 8 and 9, respectively. The magnitude correction for the rolling moment is similar to that for the side force, and the phase correction is small for most of the speed range shown. The maximum magnitude correction for the rolling moment occurs at the mid-speed range ($\mu = 0.20$), and is on the order of 40 percent reduction. Over the whole speed range, the corrected phase variation for the rolling moment is nearly identical to that of the side force. The phase correction is small except at the advance ratio of 0.15 where the corrected phase lags the uncorrected phase by roughly 90 deg. Likewise, the magnitude correction for the pitching moment exhibits a trend similar to that of the axial force with the maximum reduction of more than 50 percent; the phase variation of the corrected pitching moment is very close to that of the axial force, except for an offset of roughly 180 deg. The corrected phase of the pitching moment lags the uncorrected one by an almost uniform offset of 80-deg phase lag over the speed range shown.

CONCLUDING REMARKS

A shake test was conducted in the 40- by 80-Foot Wind Tunnel to identify the modal properties of the Large Scale Dynamic Rig and the dynamic characteristics of the installed rotor balance. Three shake test configurations were tested for hub modal identification: wind tunnel scale unlocked with dampers engaged and disengaged, and wind tunnel scale locked. Test data were analyzed with a multi-degree-of-freedom time domain algorithm to identify the modal properties of the hub mode. Test results indicate that the damping of the low frequency hub mode (ground resonance modes) increases significantly with the wind tunnel dampers engaged.

To identify the dynamic calibration of the rotor balance, the remainder of the shake test was performed only with the wind tunnel dampers engaged. The dynamic calibration matrix is computed from the test data using a least-squares error method and includes both magnitude and phase corrections for the primary as well as the interactions between the balance signals. The dynamic calibration results are then used to correct for the 5P hub loads obtained from the MDART test program. The dynamic correction reduces the side force magnitude up to two-thirds, increases the axial force magnitude up to one-half, and reduces up to one-half the magnitudes of the rolling and pitching moments. The magnitude correction for the normal force is small, less than 20 percent. The phase corrections for the side force, normal force, and rolling moment are generally small. For the axial force and pitching moment, the phase corrections are 90-deg lead and 80-deg lag, respectively.

REFERENCES

1. Gabel, R.; Sheffler, M.; Tarzanin, F.; and Hodder, D.: Wind Tunnel Modeling of Vibratory Loads. J. American Helicopter Society, vol. 28, no. 2, Apr. 1983.

2. Lehmann, G. ;and Fu, K. H.: Theoretical and Experimental Investigations on a Six-Component Rotor Balance. Proceedings of the Eleventh European Rotorcraft and Powered Lift Forum, London, England, Sept. 1983.

3. Staley, J. A.; Matthew, M. B.; and Tarzanin, F.: Wind Tunnel Modeling of High Order Rotor Vibration. Proceedings of the 49th Annual Forum of the American Helicopter Society, St. Louis, Mo., May 1993.

4. van Aken, J.; Peterson, R. L.; and Freedman, C. J.: Calibration Results of the NASA Ames Rotor Test Apparatus Steady/Dynamic Rotor Balance. American Helicopter Society Aeromechanics Specialists Conference, San Francisco, Calif., Jan. 1994.

5. Users Manual for Modal Analysis 9.0. Structural Dynamics Research Corporation, 1985.

6. Lau, B. H.; and Peterson, R. L.: Shake Test Results of the MDHC Test Stand in the 40- by 80-Foot Wind Tunnel. NASA TM-108801, Jan. 1994.

7. Kailath, T.: Linear Systems. Prentice Hall, Englewood Cliffs, N.J., 1980.

Table 1. Nodal coordinates of the stick model of the test stand shown in figure 4

	Coordinate (in.)		
Node	x	y	z
1	0	0	283.4
2	0	0	119
3	0	49	119
4	0	–49	119
5	0	49	–14
6	0	–49	–14
7	0	0	62.4
8	–118.2	0	84.7
9	–102.0	0	62.4
10	–118.2	0	–10

Table 2. Modal properties of the hub modes

	Scale		Stand						
	Long	Lat	Long 1	Lat 1	Long 2	Yaw	Long 3	Long 4	Lat 2
Dampers off									
Frequency, Hz	2.03	2.42	4.19	4.45	6.48	6.67	7.54	–	12.36
Damping, percent	6.54	3.68	1.77	1.38	0.93	0.63	1.14	–	1.02
Modal mass, slug	1813	1932	135	3136	3390	142	6618	–	167.2
Dampers on									
Frequency, Hz	–	2.94	4.26	4.64	6.57	6.71	7.78	–	12.27
Damping, percent	–	10.32	2.26	2.00	1.61	0.93	1.77	–	1.11
Modal mass, slug	–	1243	163.4	8983	3770	1386	9223	–	129.7
Locked									
Frequency, Hz	–	–	3.84	3.68	5.31	5.94	7.36	8.74	12.36
Damping, percent	–	–	0.89	1.54	1.81	3.44	2.71	3.30	1.02
Modal mass, slug	–	–	156.7	1053	573.8	344	273	4079	167.2

Table 3. Excitation sequences for dynamic calibration

Sequence	Type of shake	Hub load components				
		AF	*SF*	*NF*	*RM*	*PM*
1	Inplane	–	–1	–	–	–
2	Inplane	–1	–	–	–	–
3	Vertical (center)	–	–	1	–	–
4	Vertical (offset aft*)	–	–	1	–	–13.8
5	Vertical (offset forward*)	–	–	1	–	13.8
6	Vertical (offset right*)	–	–	1	13.8	–
7	Vertical (offset left*)	–	–	1	–13.8	–

Note: Wind tunnel dampers on.
*Viewed from above.

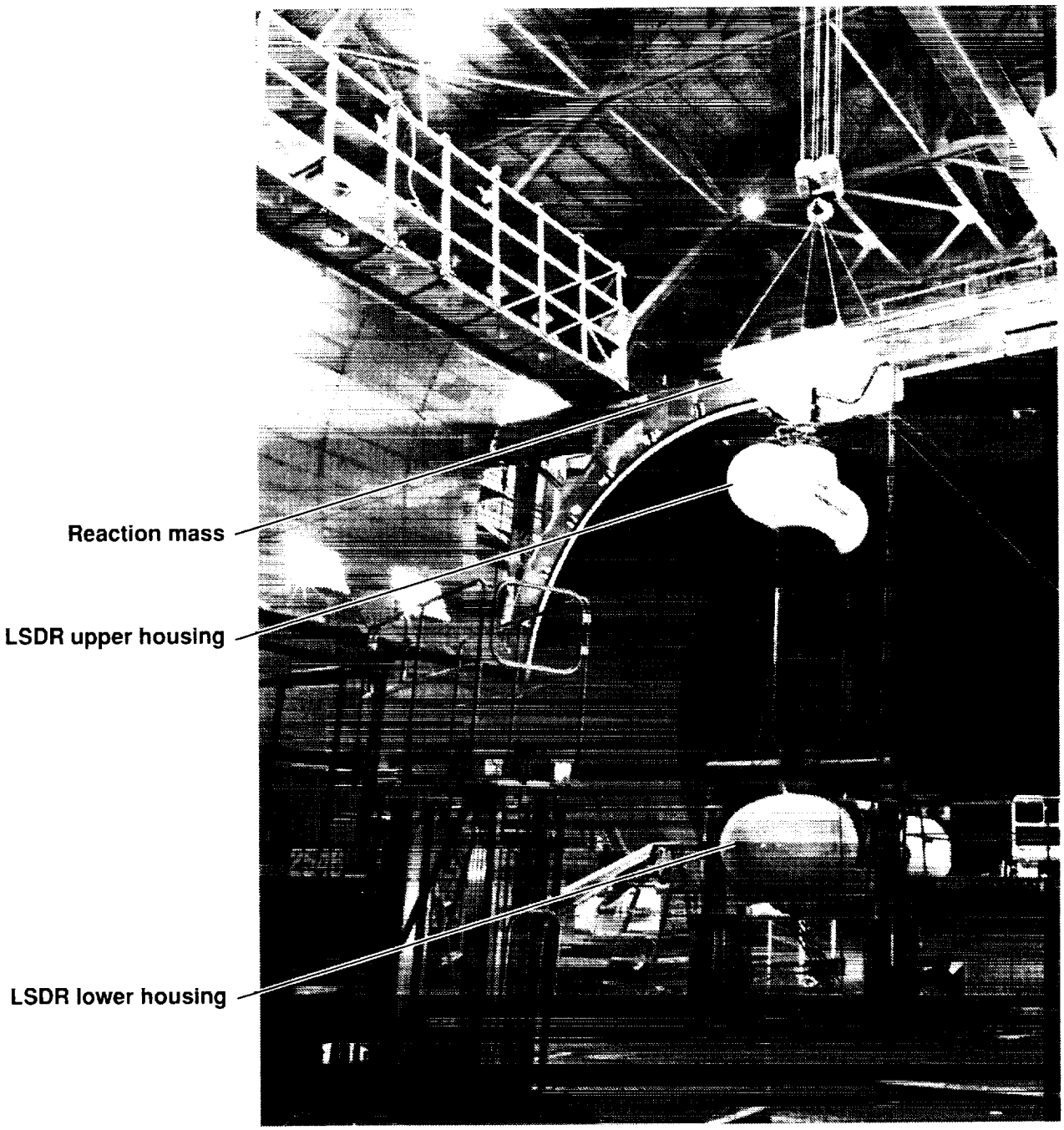

Figure 1. Shake test setup for the Large Scale Dynamic Rig in the 40- by 80-Foot Wind Tunnel.

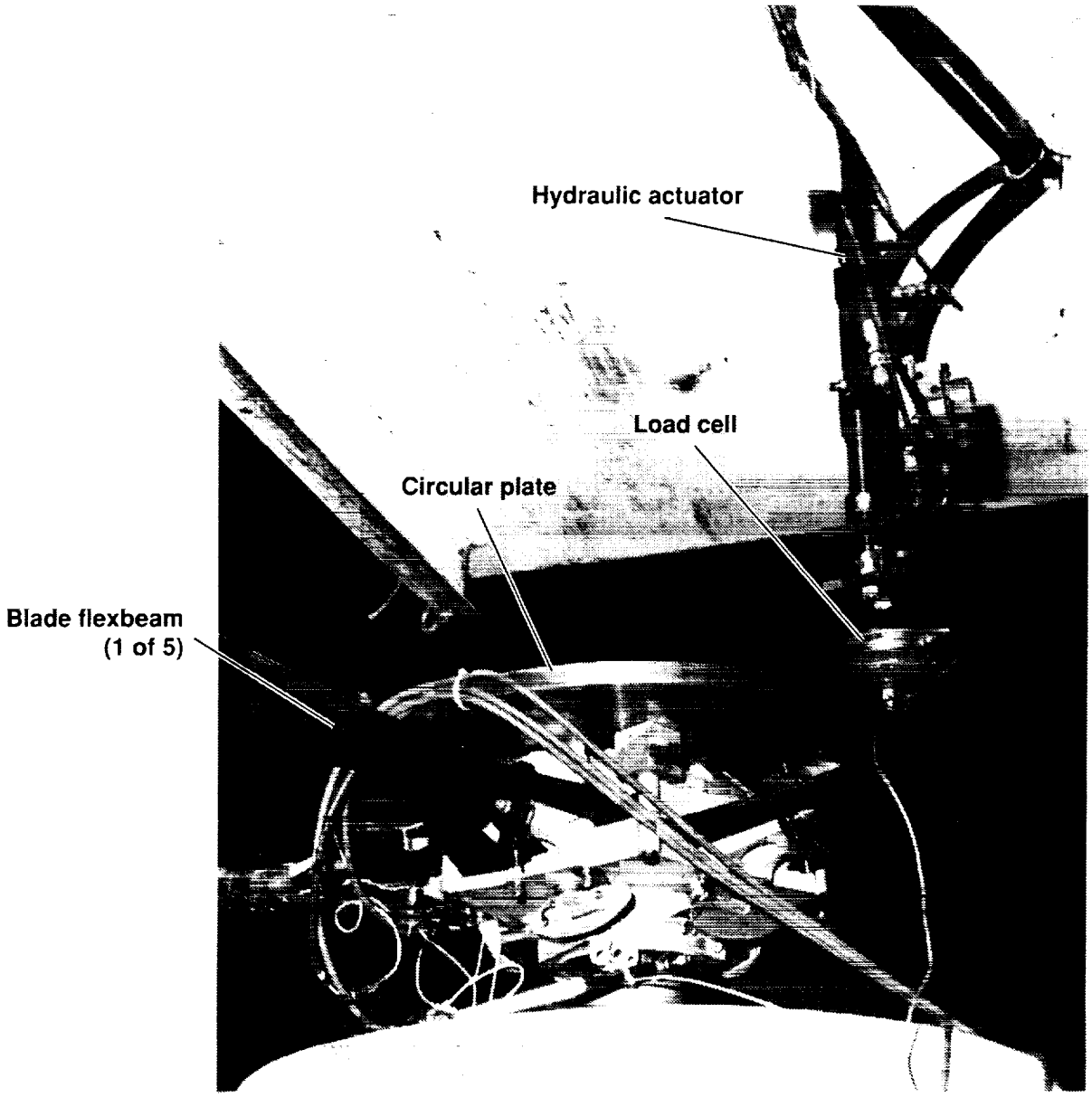

Figure 2. The Large Scale Dynamic Rig undergoing a vertical shake.

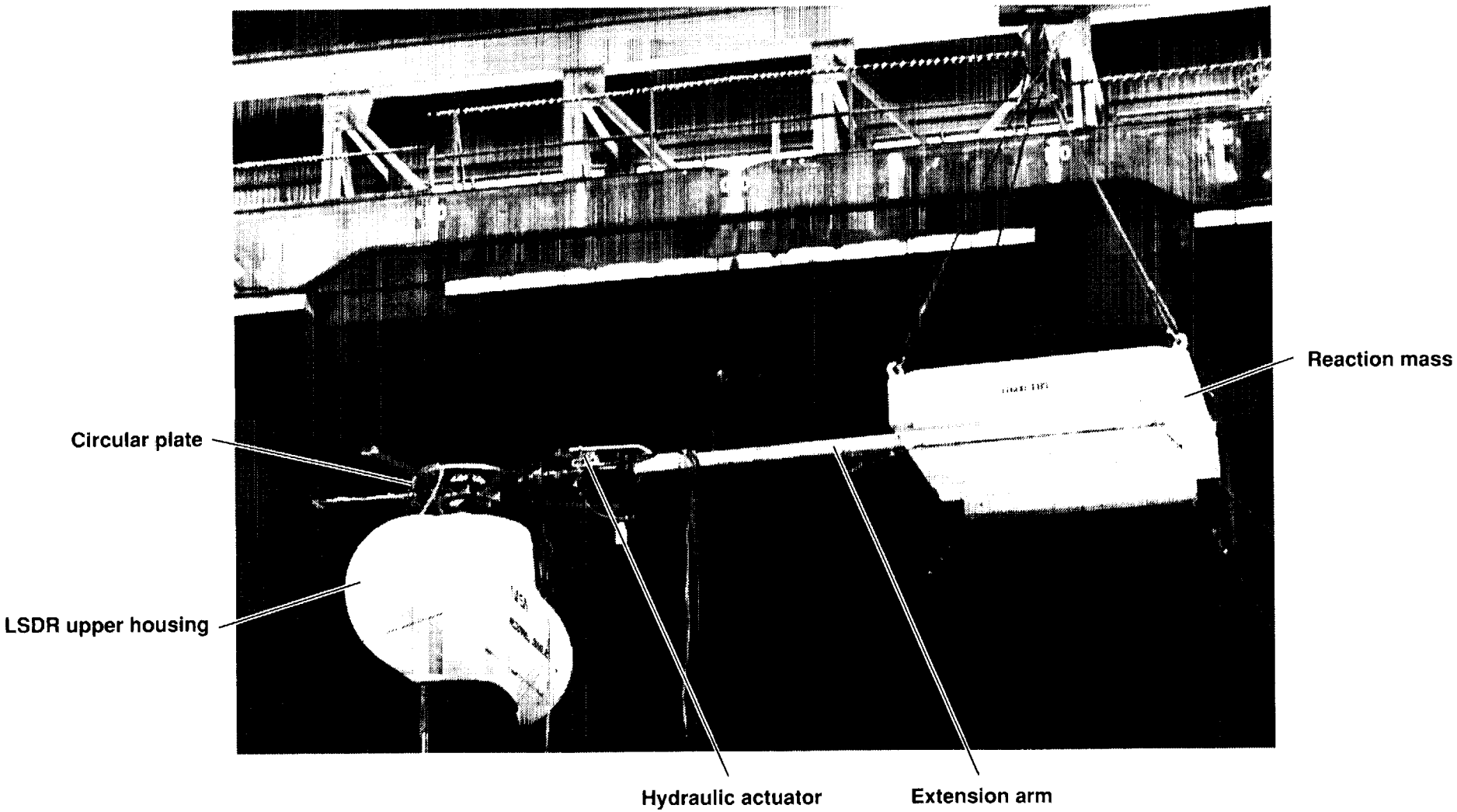

Figure 3. The Large Scale Dynamic Rig undergoing an inplane shake.

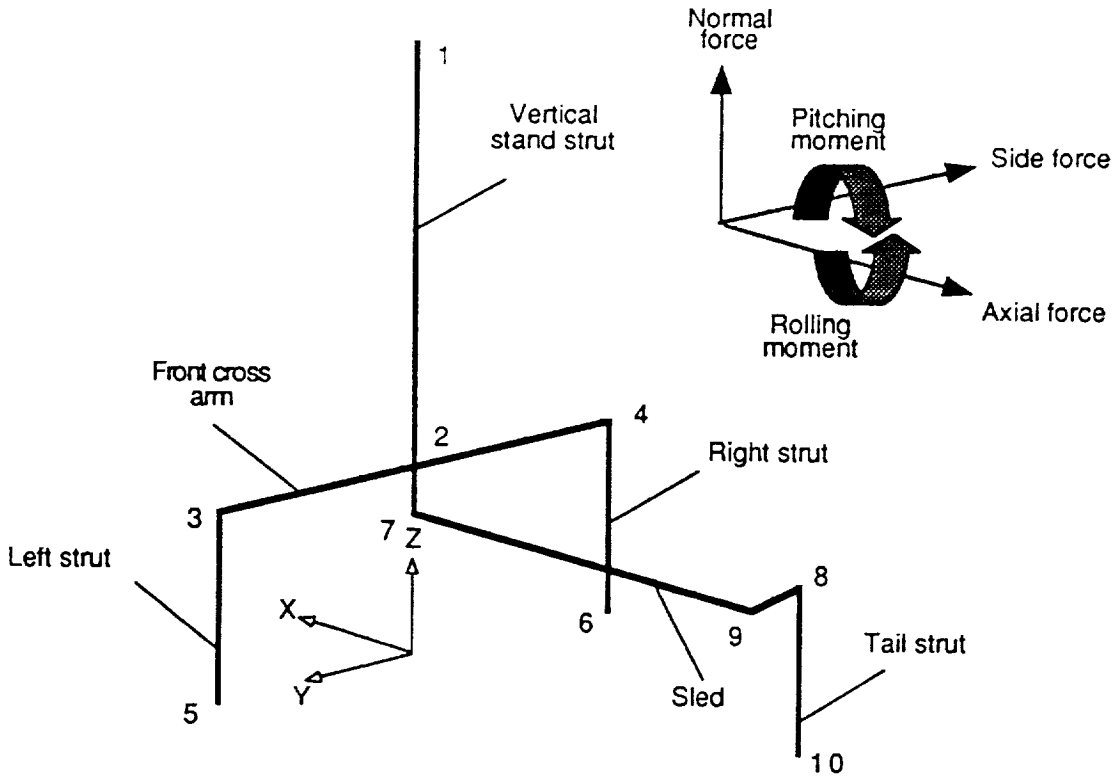

Figure 4. Stick model representation of the Large Scale Dynamic Rig for modal identification.

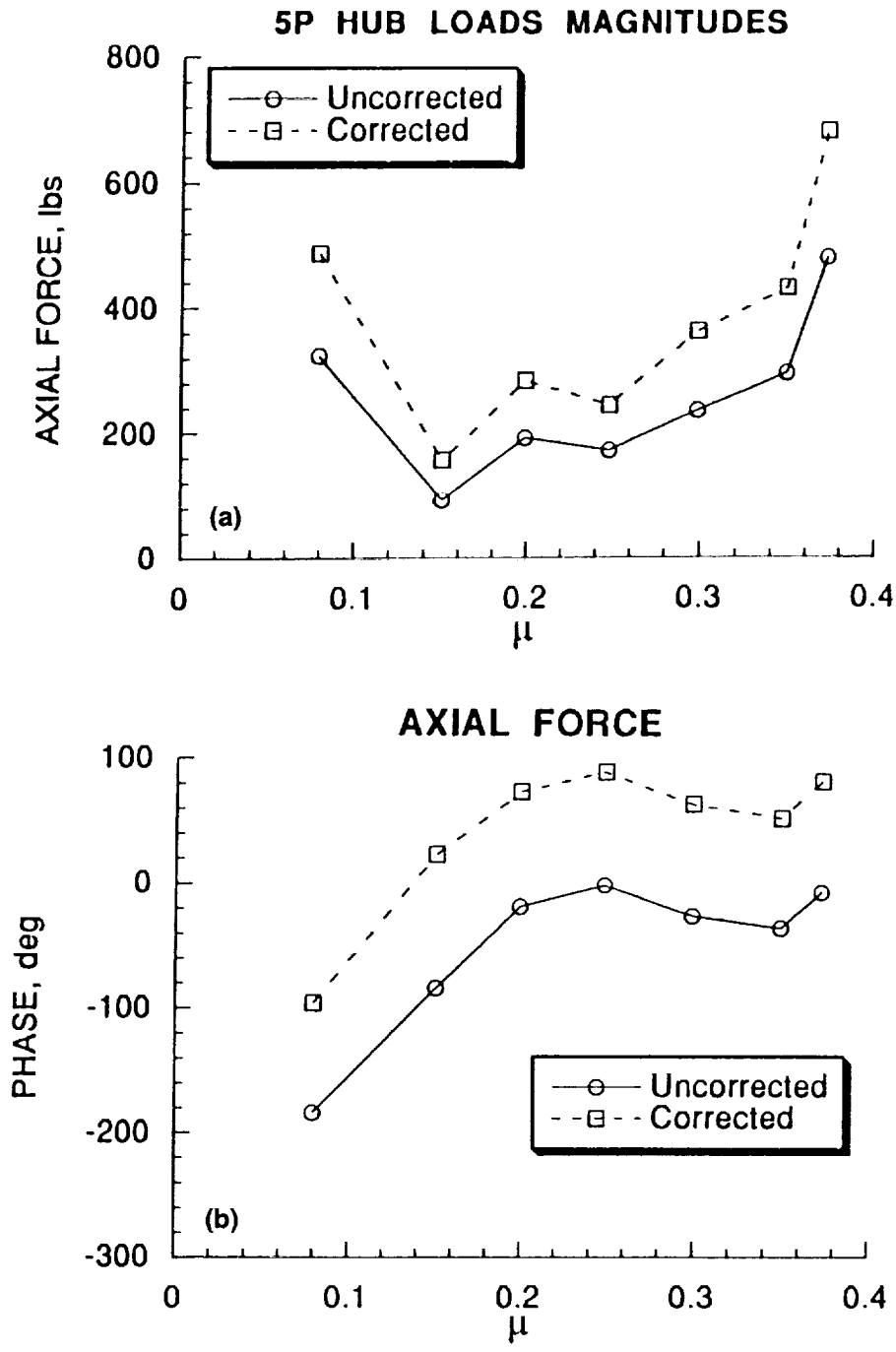

Figure 5. Variation of the dynamically corrected and uncorrected five-per-rev axial forces with advance ratio, $C_T = 0.076$. (a) Magnitude, (b) phase.

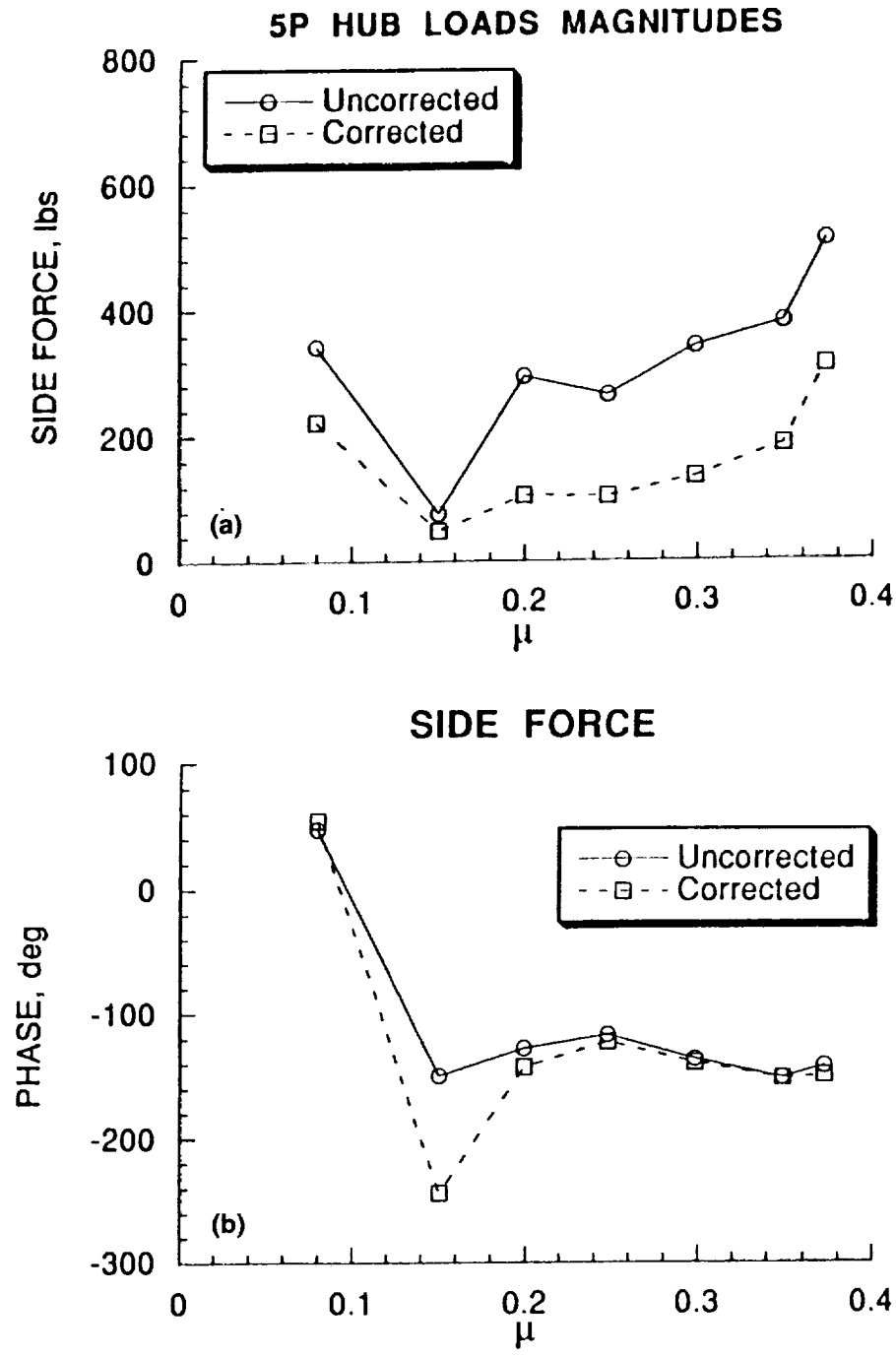

Figure 6. Variation of the dynamically corrected and uncorrected five-per-rev side forces with advance ratio, $C_T = 0.076$. (a) Magnitude, (b) phase.

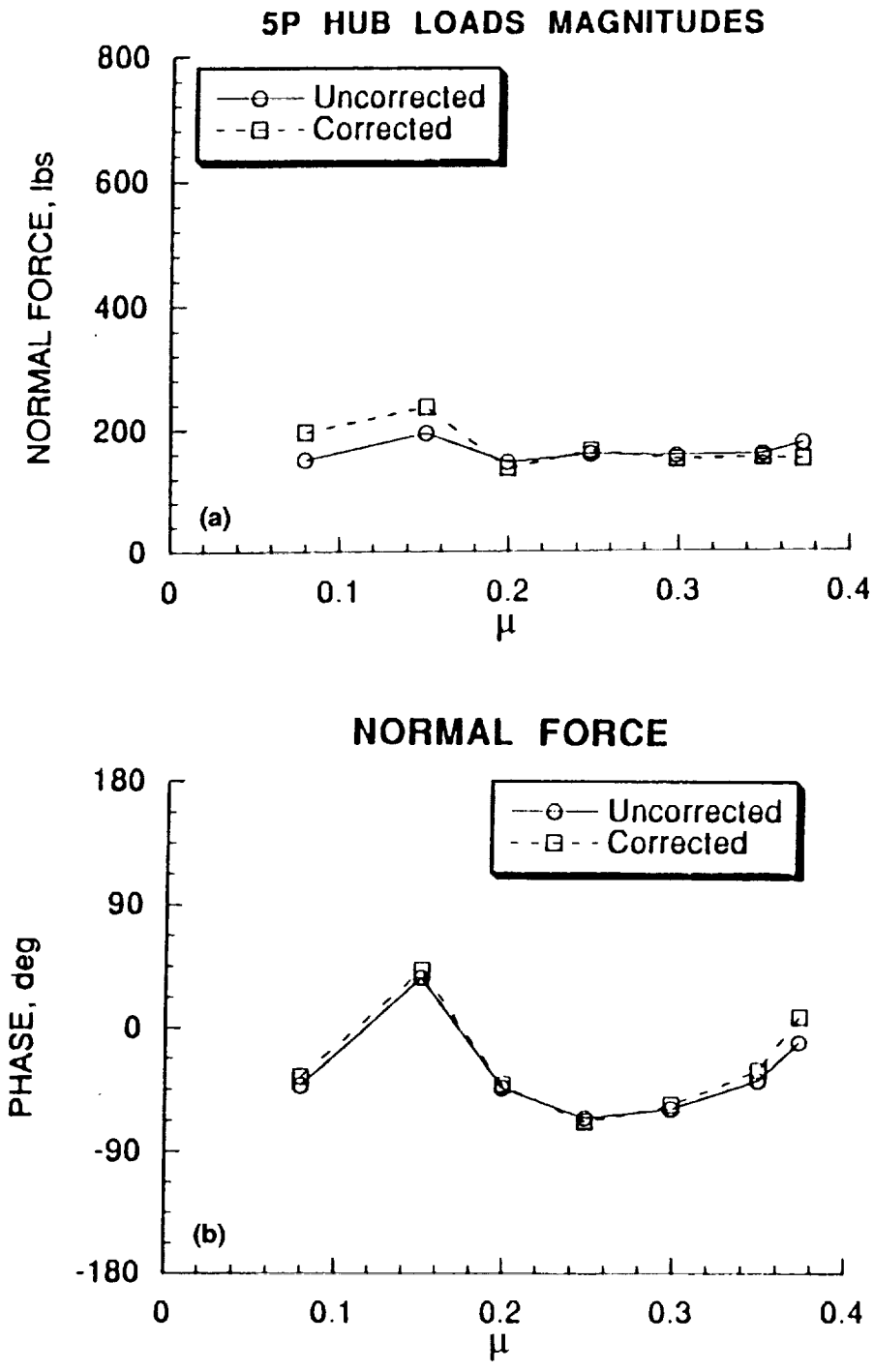

Figure 7. Variation of the dynamically corrected and uncorrected five-per-rev normal forces with advance ratio, $C_T = 0.076$. (a) Magnitude, (b) phase.

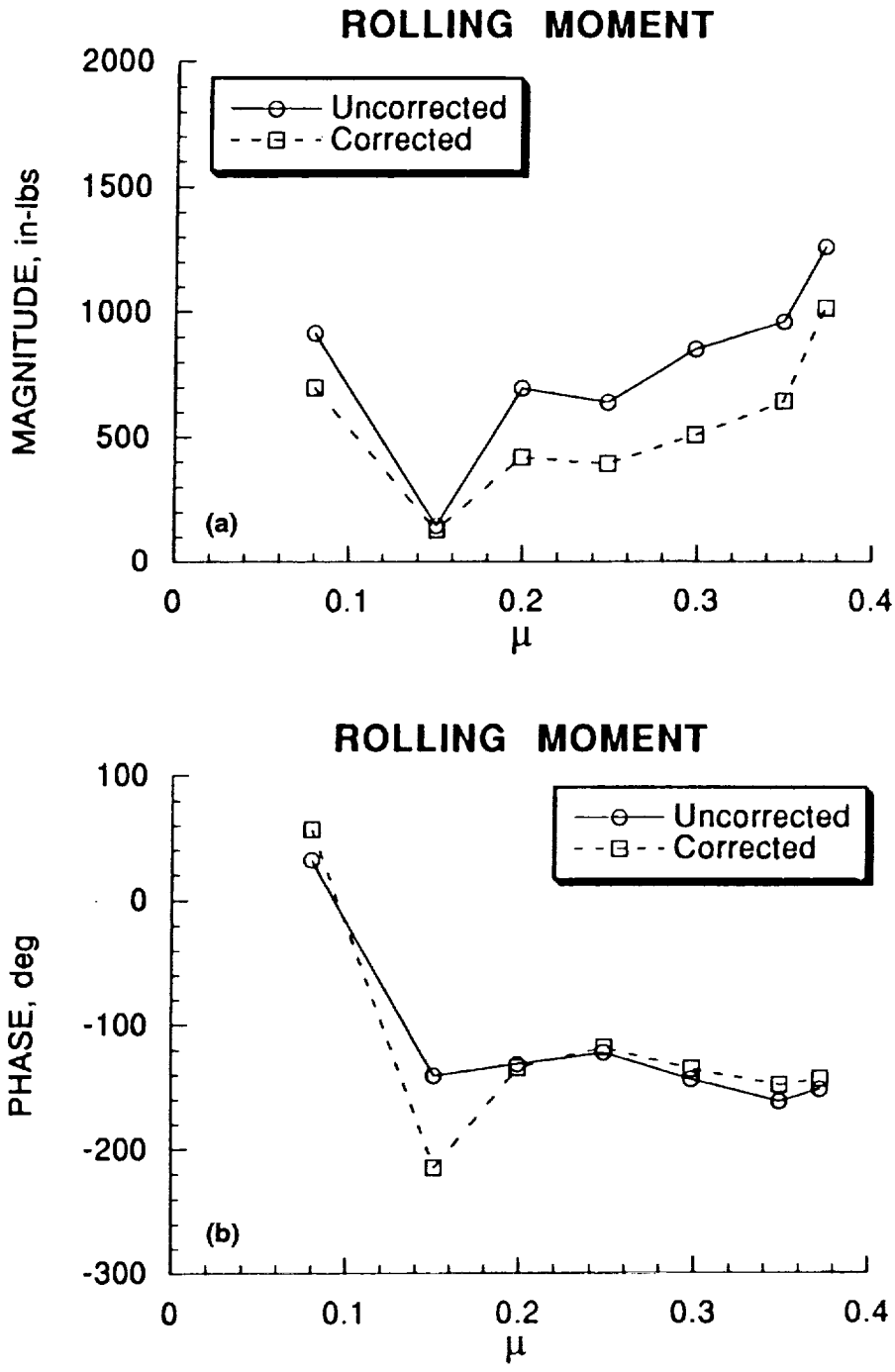

Figure 8. Variation of the dynamically corrected and uncorrected five-per-rev hub rolling moments with advance ratio, $C_T = 0.076$. (a) Magnitude, (b) phase.

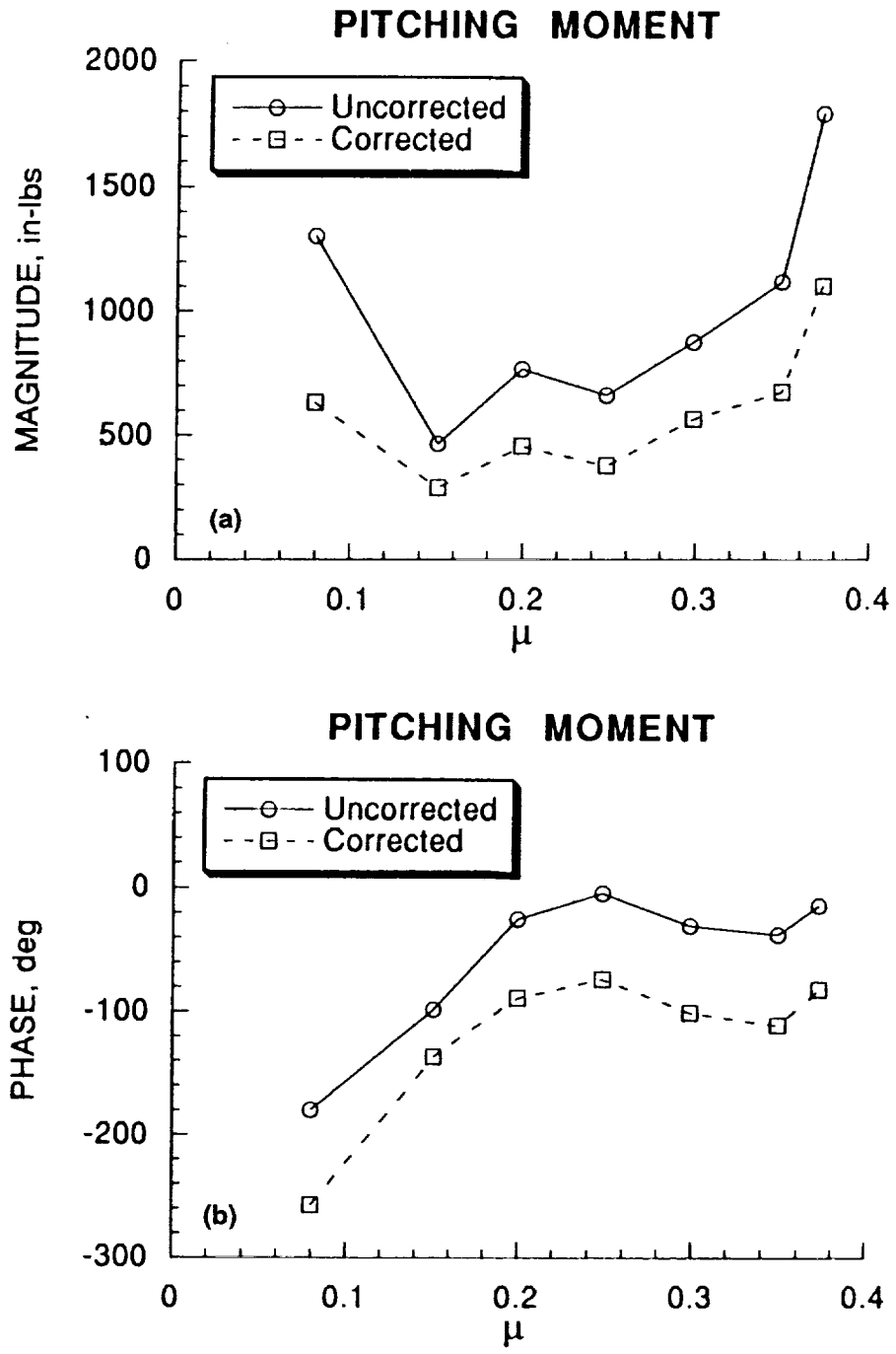

Figure 9. Variation of the dynamically corrected and uncorrected five-per-rev hub pitching moments with advance ratio, $C_T = 0.076$. (a) Magnitude, (b) phase.

REPORT DOCUMENTATION PAGE

Form Approved
OMB No. 0704-0188

1. AGENCY USE ONLY *(Leave blank)*	2. REPORT DATE	3. REPORT TYPE AND DATES COVERED
	October 1994	Technical Memorandum

4. TITLE AND SUBTITLE
Dynamics of the McDonnell Douglas Large Scale Dynamic Rig and Dynamic Calibration of the Rotor Balance

5. FUNDING NUMBERS
505-59-36

6. AUTHOR(S)
Khanh Nguyen and Benton Lau

7. PERFORMING ORGANIZATION NAME(S) AND ADDRESS(ES)
Ames Research Center
Moffett Field, CA 94035-1000

8. PERFORMING ORGANIZATION REPORT NUMBER
A-94007

9. SPONSORING/MONITORING AGENCY NAME(S) AND ADDRESS(ES)
National Aeronautics and Space Administration
Washington, DC 20546-0001

10. SPONSORING/MONITORING AGENCY REPORT NUMBER
NASA TM-108855

11. SUPPLEMENTARY NOTES
Point of Contact: Khanh Nguyen, Ames Research Center, MS T12-B, Moffett Field, CA 94035-1000; (415) 604-5043

12a. DISTRIBUTION/AVAILABILITY STATEMENT
Unclassified — Unlimited
Subject Category 01

12b. DISTRIBUTION CODE

13. ABSTRACT ***(Maximum 200 words)***

A shake test was performed on the Large Scale Dynamic Rig in the 40- by 80-Foot Wind Tunnel in support of the McDonnell Douglas Advanced Rotor Technology (MDART) Test Program. The shake test identifies the hub modes and the dynamic calibration matrix of the rotor balance. For hub mode identification, three configurations were tested: wind tunnel scale unlocked with dampers engaged and disengaged, and wind tunnel scale locked. Test data were analyzed with a multi-degree-of-freedom time domain algorithm to identify the modal properties of the hub modes. The damping of the low frequency hub modes (ground resonance modes) increases significantly with the wind tunnel dampers engaged. For dynamic calibration of the rotor balance, the shake test was performed only with the wind tunnel dampers engaged. The dynamic calibration matrix, computed from the shake test data using a least squares error method, is used to correct the five-per-rev vibratory balance readings. The corrections are large for the side force, moderate for the axial force and inplane hub moments, and small for the normal force.

14. SUBJECT TERMS
Dynamic calibration, Shake test, Hub mode identification

15. NUMBER OF PAGES
28

16. PRICE CODE
A03

17. SECURITY CLASSIFICATION OF REPORT	18. SECURITY CLASSIFICATION OF THIS PAGE	19. SECURITY CLASSIFICATION OF ABSTRACT	20. LIMITATION OF ABSTRACT
Unclassified	Unclassified		